Biochimica et Biophysica Acta 1840 (2014) 1171–1180

Contents lists available at ScienceDirect

Biochimica et Biophysica Acta

journal homepage: www.elsevier.com/locate/bbagen

Physicochemical properties and in vitro intestinal permeability properties and intestinal cell toxicity of silica particles, performed in simulated gastrointestinal fluids

Kumiko Sakai-Kato [a,*], Masayuki Hidaka [a], Keita Un [a], Toru Kawanishi [b], Haruhiro Okuda [b]

[a] Division of Drugs, National Institute of Health Sciences, 1-18-1 Kamiyoga, Setagaya-ku, Tokyo 158-8501, Japan
[b] National Institute of Health Sciences, 1-18-1 Kamiyoga, Setagaya-ku, Tokyo 158-8501, Japan

ARTICLE INFO

Article history:
Received 11 July 2013
Received in revised form 10 December 2013
Accepted 13 December 2013
Available online 19 December 2013

Keywords:
Nanomaterial
Silica particle
In vitro model
Simulated gastrointestinal fluid

ABSTRACT

Background: Amorphous silica particles with the primary dimensions of a few tens of nm, have been widely applied as additives in various fields including medicine and food. Especially, they have been widely applied in powders for making tablets and to coat tablets. However, their behavior and biological effects in the gastrointestinal tracts associated with oral administration remains unknown.
Methods: Amorphous silica particles with diameters of 50, 100, and 200 nm were incubated in the fasted-state and fed-state simulated gastric and intestinal fluids. The sizes, intracellular transport into Caco-2 cells (model cells for intestinal absorption), the Caco-2 monolayer membrane permeability, and the cytotoxicity against Caco-2 cells were then evaluated for the silica particles.
Results: Silica particles agglomerated in fed-state simultaneous intestinal fluids. The agglomeration and increased particles size inhibited the particles' absorption into the Caco-2 cells or particles' transport through the Caco-2 cells. The in vitro cytotoxicity of silica particles was not observed when the average size was larger than 100 nm, independent of the fluid and the concentration.
Conclusion: Our study indicated the effect of diet on the agglomeration of silica particles. The sizes of silica particles affected the particles' absorption into or transport through the Caco-2 cells, and cytotoxicity in vitro, depending on the various biological fluids.
General significance: The findings obtained from our study may offer valuable information to evaluate the behavior of silica particles in the gastrointestinal tracts or safety of medicines or foods containing these materials as additives.

1. Introduction

Nanomaterials are materials that have at least one dimension in the nanoscale range (approximately 1 nm to 100 nm). Recently, nanomaterials have been applied in various fields, including medicine, cosmetics, and foods, because nanomaterials may have physical, chemical, or biological properties that are different from those of their bulk. While nanotechnology can exploit the improved and often novel properties of materials, there have been publications about concerns regarding the safety to humans and potential environmental impact of such materials [1–4].

In the medical field, nanomaterials have been used as drug carriers for drug delivery systems (DDS) [5–8].

Amorphous silica particles have been widely applied as additives for various purposes, for example, to improve the flowability used in powders for making tablets; they have also been applied as additives to coat tablets, to improve their hardness. In solid oral dosage form, silicates are often used as glidants. Glidants are substances that improve the flowability of cohesive powders and granules. Silicates are well suited for that purpose, because of their small particle size and large specific surface area. One of the most frequently used glidants is colloidal silica (e.g., Aerosil 200), which exhibits very small particle sizes in the nanometer range, and a large specific surface area of approximately 200 m^2/g [9]. Although the primary dimensions of these particles are a few tens of nm, they form aggregates of a few hundred nm. These novel materials have been the focus of medical developments in a number of areas, and many researchers have investigated their use not only as additives in tablets, but also as novel carriers for poorly-water-soluble drugs [10–12].

Amorphous silica particles have also been used in other fields, where they are applied directly to the human body as ingredients in cosmetics and toothpaste, or even as powdered food ingredients to prevent caking [13,14].

Abbreviations: DDS, drug delivery system; PDI, polydispersity index; TEM, transmission electron microscopy; FaSSGF, fasted-state simulated gastric fluids; FeSSGF, fed-state simulated gastric fluids; FaSSIF, fasted-state simulated intestinal fluids; FeSSIF, fed-state simulated intestinal fluids; DMEM, Dulbecco's modified Eagle's medium; PBS, Phosphate buffer saline; HBSS, Hanks' balanced salt solution; FBS, fetal bovine serum; TEER, transepithelial electrical resistance

* Corresponding author. Tel./fax: +81 3 3700 9662.
E-mail address: kumikato@nihs.go.jp (K. Sakai-Kato).

0304-4165/$ – see front matter © 2013 Elsevier B.V. All rights reserved.
http://dx.doi.org/10.1016/j.bbagen.2013.12.014

However, when amorphous silica particles were swabbed on skin, it was reported that the nano-sized materials penetrated through the skin, became distributed in the body, and induced unexpected toxicity [2]. It has been reported that the toxicity derived from amorphous silica particles depends on the particle size and the surface properties [15,16].

Generally, tablets are taken via oral administration. Using this administration route, the particles contained in the tablets do not remain at specific sites for a long period. However, if the particles are absorbed from the intestine and enter the blood circulation, it is important to consider whether the phenomena that occur when the drugs are administered intravenously would also occur in this case. In addition, no studies have been performed to investigate the toxicity associated with the oral administration of amorphous silica particles as additives in oral solid dosage forms; the evaluation of the physicochemical properties, intestinal permeability properties, and intestinal cell toxicity resulting from the oral administration of nano- or submicron-size amorphous silica particles is therefore essential to ensure the safety of solid oral dosage forms containing these materials.

In the present study, we evaluated the size, the absorption from the intestine, and the cytotoxicity using in vitro models of amorphous silica particles after oral administration. In particular, we investigated the effects of the size of the particles and the composition of the intestinal tract fluid on the intestinal permeability properties and the intestinal cell toxicity. In this study, we used amorphous silica particles with diameters of 50, 100, and 200 nm. In the oral administration of medicines, the physiological conditions in the intestinal tract are dramatically different in the fasted state and the fed state. It is known that these differences affect the absorption of drugs from the gastrointestinal tract. This study therefore investigated the changes in the size of amorphous silica particles in the fasted-state and fed-state simulated gastric and intestinal fluids.

As an in vitro model for intestinal absorption, we used the Caco-2 cell. Caco-2 cells grown as a monolayer become differentiated and polarized such that their morphological and functional phenotype resembles that of the enterocytes that line the small intestine [17,18]. Caco-2 cells express tight junctions, microvilli, and numerous enzymes and transporters that are characteristic of such enterocytes. The Caco-2 monolayer is widely used throughout the pharmaceutical industry as an in vitro model of the human small intestinal mucosa to predict the absorption of orally administered drugs. The correlation between the in vitro apparent permeability across Caco-2 monolayers and the in vivo fraction absorbed is well established [19]. Caco-2 cells have in fact been used as a model to investigate the possible harmful effect of silica nanoparticles in the gastrointestinal tract [20]. Furthermore, Caco-2 monolayers have been used to evaluate the intracellular uptake of nanosized-drug delivery systems [21,22].

In this study, the intracellular transport into Caco-2 cells, the Caco-2 monolayer membrane permeability, and the cytotoxicity against Caco-2 cells were then evaluated for the amorphous silica particles, in the fasted-state and fed-state simulated gastric and intestinal fluids.

2. Materials and methods

2.1. Silica particles

Suspensions of fluorescently labeled amorphous silica particles (nominal diameters as stated by suppliers: 50 nm, SP-50; 100 nm, SP-100; and 200 nm, SP-200) were obtained from Micromod Partikeltechnologie (Rostock, Germany). These were amorphous silica particles [16]. Silica suspensions were shaded and stored at 4 °C and diluted in various fluids before each experiment. The suspensions were sonicated for 10 min, and then vortexed for 1 min immediately prior to use. The silica particles were suspended in various fluids, and then incubated at 37 °C for 1 h before the measurements were performed. The mean particle size, the polydiversity index (PDI), and the ζ-potentials of the silica particles were measured using a Zetasizer Nano-ZS (Malvern Instruments, UK), with a concentration of 0.1 mg/mL in water (Table 1). The water used in this study was purified using Milli-Q system (Millipore, Tokyo, Japan). Fig. 1 shows transmission electron microscopy (TEM) images of the silica particles used in this study. The images were obtained using an H-9000 UHR instrument (Hitachi, Tokyo, Japan).

Table 1
The mean particle size, the polydiversity index (PDI), and the ζ-potentials of the silica particles used in this study.

Sample	Particle size (nm)	PDI	ζ-Potential
Silica			
SP-50	47.5 ± 4.0	0.14 ± 0.053	−43.2 ± 2.0
SP-100	99.0 ± 3.2	0.03 ± 0.030	−53.8 ± 1.4
SP-200	176 ± 6.4	0.16 ± 0.024	−51.8 ± 1.4

Samples were dissolved in MilliQ water with a concentration of 0.1 mg/mL.
Each value represents the mean ± S.D. ($n = 3$).

2.2. Cell culture

Caco-2 cells—human epithelial colorectal adenocarcinoma cells (American Type Culture Collection (ATCC), Manassas, VA, USA)—were cultured in Dulbecco's modified Eagle's medium (Life Technologies, Brooklyn, NY, USA) supplemented with 10% FBS (Nichirei Biosciences, Tokyo, Japan), 100 U/ml penicillin/streptomycin (Life Technologies). Cells were grown in a humidified incubator at 37 °C under 5% CO_2, and the culture medium was changed every other day.

2.3. Composition of simulated gastric and intestinal fluids

The fasted-state simulated gastric fluids (FaSSGF) and the fed-state simulated gastric fluids (FeSSGF) were prepared according to a previous report [23]. The fasted-state simulated intestinal fluids (FaSSIF) and the fed-state simulated intestinal fluids (FeSSIF) were prepared according to the manufacturer's instructions (Celeste Co., Tokyo, Japan). An Ubbelohde-type viscometer was used for the viscosity measurements. The detailed components of each fluid are shown in Table 2.

2.4. Stability of fluorescence labeling

Fluorescently labeled silica particles were diluted to 1 mg/mL in various types of fluids (MilliQ water, D-MEM, PBS, FaSSIF, FeSSIF, FaSSGF, FeSSGF, 0.25% trypsin-ethylenediamine tetraacetic acid, and lysis buffer (1.0% Triton X-100 in HBSS)) and incubated at 37 °C for 6 h. After incubation, the particles were centrifuged (20,000 g, 30 min) and the precipitated silica particles were resuspended with the same volumes of fresh fluids as those before centrifugation. The fluorescent intensities of the suspension before and after centrifugation were measured at an excitation wavelength of 542 nm and an emission wavelength of 602 nm in a fluorescence spectrophotometer (F-7000; Hitachi High-Technologies, Tokyo, Japan). The percentage of the fluorescent dye retained in the silica particles after 6-h incubation was expressed as follows:

$$A/B \times 100(\%),$$

where A represents the fluorescence intensity of the silica particles resuspended with fresh fluid after centrifugation, and B represents the fluorescence intensity of the silica suspension before centrifugation.

2.5. Intracellular uptake study

Fluorescently labeled silica particles were used in this study to evaluate the intracellular uptake of silica particles. Caco-2 cells (1×10^6) were plated in a 6-well plate in medium containing 10% FBS and 100 U/mL penicillin/streptomycin. The fluorescently labeled silica particles were diluted to a concentration of 0.1 mg/mL in various types of fluids (D-MEM, PBS, FaSSIF, and FeSSIF), and then incubated at 37 °C for 1 h to mimic the intestinal conditions. In addition, to mimic the

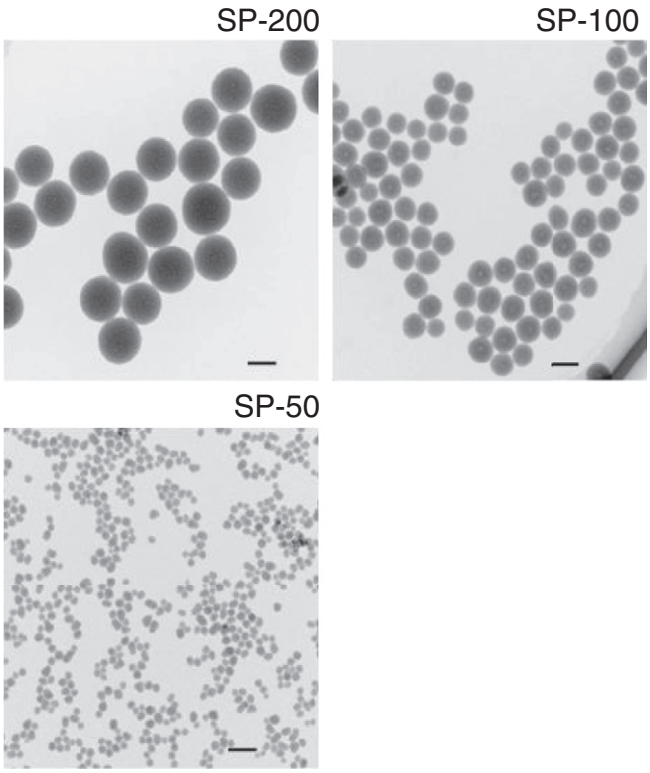

Fig. 1. TEM images of silica particles used in this study. The scale bar represents 100 nm.

gastric and intestinal conditions (indicated as "FaSSGF → FaSSIF" and "FeSSGF → FeSSIF"), fluorescently labeled silica particles were diluted to 10 mg/mL in FaSSGF or FeSSGF, and incubated at 37 °C for 1 h. Subsequently, the diluted silica particles were further diluted to a concentration of 0.1 mg/mL in FaSSIF or FeSSIF, and incubated at 37 °C for an additional 1 h. The diluted and incubated fluorescently labeled silica particles were added to the cells, which were pre-incubated for 96 h (37 °C, 5% CO_2). After incubation for 2 h in the silica particle-containing fluid, the cells were washed, and the incubation medium was replaced with Hanks' balanced salt solution (HBSS). The cells were then trypsinized with 0.25% trypsin-ethylenediamine tetraacetic acid (Life Technologies), washed with HBSS three times, and suspended in lysis buffer (1.0% Triton X-100 in HBSS). The cell suspension was shaken, centrifuged at 15,000 ×*g* and 4 °C for 10 min, and the fluorescence intensity of the resulting supernatant was measured at an excitation wavelength of 542 nm and an emission wavelength of 602 nm in a fluorescence spectrophotometer (F-7000). The fluorescence intensity was expressed as incorporated particle mass per unit protein content of cells. The protein concentration was determined using a protein assay kit (Dojindo Molecular Technologies, Tokyo, Japan).

Table 2
Composition of FaSSGF, FeSSGF, FaSSIF, and FeSSIF.

	FaSSGE	FeSSGF	FaSSIF	FeSSIF
Sodium taurocholate (μM)	80	–	3	15
Sodium acetate (mM)	–	29.75	–	–
Sodium chloride (mM)	34.2	237.02	105.4	203.1
Sodium hydroxide (mM)	–		10.5	101
Sodium dihydrogen-orthophosphate (mM)			28.7	
Acetic acid (mM)		17.12	–	144.17
Lecithin (μM)	20	–	0.75	3.75
Pepsin (mg/mL)	0.1	–	–	–
pH	1.6	5	6.5	5.0
Osmolality (mOsm/kg)	120.7 ± 2.5	400	270 ± 10	635 ± 10

2.6. Confocal microscopy study

To observe the intracellular uptake of the fluorescently labeled silica particles, Caco-2 cells (5.0×10^4) were plated in 35 mm glass-bottom dishes coated with poly-L-lysine (Matsunami Glass, Osaka, Japan) in medium containing 10% FBS and 100 U/mL penicillin/streptomycin. The fluorescently labeled silica particles were diluted to a concentration of 0.1 mg/mL in various types of fluids (PBS, FaSSIF, and FeSSIF), and then incubated at 37 °C for 1 h to mimic the intestinal conditions. After the cells were pre-incubated for 48 h (37 °C, 5% CO_2), the diluted and incubated fluorescently labeled silica particles were added to the cells. After incubation for 2 h in the silica particle-containing fluid (37 °C or 4 °C, 5% CO_2), the cells were washed and kept in HBSS for imaging using confocal microscopy (Carl Zeiss LSM 510, Oberkochen, Germany). To observe co-localization, endosomes and lysosomes of cells were labeled with AlexaFluor-488-conjugated transferrin (Life Technologies) and LysoTracker Green DND-26 (Life Technologies), respectively, in accordance with the manufacturer's instructions. Data were collected using dedicated software supplied by the manufacturers, and exported in tagged image file format.

2.7. Transcellular transport study

Caco-2 cells were suspended in a serum-free medium consisting of D-MEM and Mito + Serum Extender (BD Biosciences, San Jose, CA, USA), and seeded on 24-well size BD Falcon cell culture inserts (BD Biosciences) at 2×10^5 cells/well [24]. In experiments that required the use of differentiation medium, the seeding medium was replaced with optimized differentiation medium 48 h after cell seeding; the medium was replaced every 24 h thereafter. The transepithelial electrical resistance (TEER) was also measured using a Millicell-ERS resistance system (Millipore, Billerica, MA, USA) every 24 h, and the wells with TEER values of over 200 Ω cm^2 were used as Caco-2 cell monolayers. The fluorescently labeled silica particles were diluted to a concentration of 1 mg/mL in various types of fluids (PBS, FaSSIF, and FeSSIF), and then incubated at 37 °C for 1 h to mimic the intestinal conditions. In addition, to mimic the gastric and intestinal conditions (indicated as "FaSSGF → FaSSIF" and "FeSSGF → FeSSIF"), fluorescently labeled silica particles were diluted to 10 mg/mL in FaSSGF or FeSSGF, and incubated at 37 °C for 1 h. The diluted silica particles were subsequently further diluted to a concentration of 1 mg/mL in FaSSIF or FeSSIF, and incubated at 37 °C for an additional 1 h. The diluted and incubated fluorescently labeled silica particles were added to the apical side of the Caco-2 cell monolayers. Phosphate buffer saline (PBS) was added to the basal side at the same time. Samples (fluorescently labeled silica particles) were drawn out of the basal side at 15 min intervals. An equal volume of PBS was added to the basal side immediately after each sampling. The TEER was simultaneously determined using a Millicell-ERS resistance system.

2.8. Cytotoxicity study

The cytotoxicity of the silica particles was assessed using a WST-8 assay (Cell Counting Kit-8, Dojindo Laboratories, Kumamoto, Japan). Caco-2 cells (1×10^5) were plated in 96-well plate in medium containing 10% FBS and 100 U/mL penicillin/streptomycin. Silica particles were diluted to concentrations of 0.1, 1, or 10 mg/mL in various types of fluids (D-MEM, PBS, FaSSIF, and FeSSIF), and incubated at 37 °C for 1 h to mimic the intestinal conditions. In addition, to mimic the gastric and intestinal conditions (indicated as "FaSSGF → FaSSIF" and "FeSSGF → FeSSIF"), silica particles were diluted to 10 mg/mL in FaSSGF or FeSSGF, and incubated at 37 °C for 1 h. The diluted silica particles were subsequently further diluted to concentrations of 0.1 or 1 mg/mL in FaSSIF or FeSSIF, and incubated at 37 °C for an additional 1 h. After the cells were pre-incubated for 72 h (37 °C, 5% CO_2), the diluted and subsequently incubated particles were added to the cells. After

incubation for 6 h, the cells were washed, the fluid was replaced with fresh culture medium without silica particles, and an additional 0, 6, 24, or 48 h of incubation was applied. Cell counting kit-8 solutions were then added to each well, and the cells were incubated for 2 h. After incubation, absorbance values at 450 nm were measured using a microplate reader (Bio-Rad Laboratories, Hercules, CA, USA), and the results were expressed as viability (%).

2.9. Statistical analyses

The results are presented here as the mean ± S.D., calculated from more than three experiments. An analysis of variance (ANOVA) was used to test the statistical significance of the differences between groups. Multiple comparisons between control and test groups were performed using Dunnett's test.

3. Results

3.1. Effects of simulated gastric and intestinal fluids on the size of silica particles

The effects of various fluids on the size of the amorphous silica particles were evaluated. Following the dispersion of the silica particle samples (nominal diameters: 50 nm, SP-50; 100 nm, SP-100; and 200 nm, SP-200, as stated by the supplier) SP-50, SP-100 and SP-200 in MilliQ water, the mean particle sizes were approximately 48 nm, 99 nm, and 176 nm, respectively (Table 1), which agreed well with the nominal diameters as stated by the supplier. The ζ-potentials of the silica particles ranged from −43.2 to −53.8 mM (Table 1). Then, to investigate how the state of the silica particles changed after oral administration, and during their passage through the gastrointestinal tract, the silica particles were dispersed in various types of simulated fluids. As shown in Fig. 2, when these silica particles were dispersed in fasted- and fed-state simulated gastric fluids (FaSSGF and FeSSGF) and fasted-state simulated intestinal fluids (FaSSIF), the mean particle sizes of SP-50, SP-100, and SP-200 were not affected. By contrast, when the silica particles were dispersed in fed-state simulated intestinal fluids (FeSSIF), the mean measured particle sizes of SP-50, SP-100, and SP-200 all significantly increased, to more than 1000 nm (Fig. 2). In addition, the PDI values of the silica particles dispersed in FeSSIF also increased to approximately 0.6, indicating that the SP-50, SP-100, and SP-200 particles all agglomerated in FeSSIF, regardless of the primary particle size. Then, to investigate conditions more similar to those encountered in actual oral administration before the passage through the intestinal tract, the silica particles were first diluted with simulated gastric fluids; this was then followed by dispersion in simulated intestinal fluids. As shown in Fig. 2, when the silica particles were dispersed in fasted-state simulated fluids (FaSSGF and FaSSIF), the mean particle sizes of SP-50, SP-100, and SP-200 were not affected. By contrast, when SP-50, SP-100, and SP-200 were dispersed in fed-state simulated fluids (FeSSGF and FeSSIF), the mean measured particle sizes increased to more than 1000 nm (Fig. 2). These results suggested that silica particles—at least those used in this study—would agglomerate after postprandial oral administration.

3.2. Stability of fluorescent labeling of silica particles

The intracellular uptake and transcellular transport assay of silica particles depend on the accuracy of the measured fluorescence. The studies supporting stability of fluorescent labeling were performed. After incubation of fluorescently labeled silica particles in various fluids, the recovery of fluorescent dye was examined. As shown in Table 3, the fluorescent labeling of silica particles used in this study was stable in every fluid under the conditions used in this study.

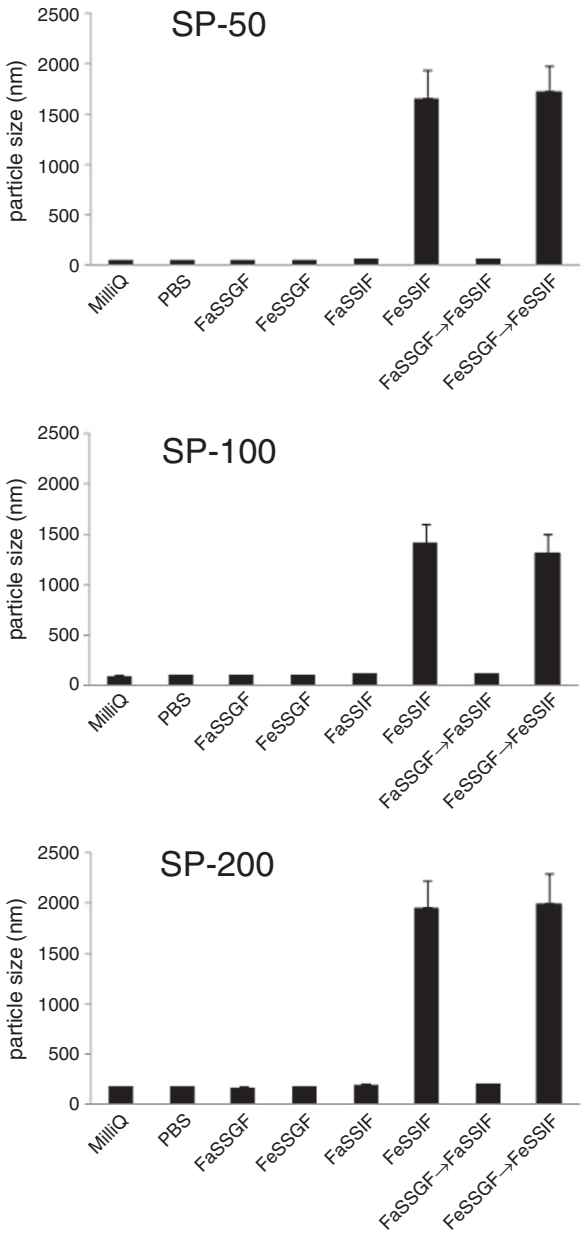

Fig. 2. Sizes of amorphous silica particles (SP-50, 100, and 200, 0.1 mg/mL) in various types of fluids. The mean particle size of the silica particles was measured using a Zetasizer Nano-ZS (Malvern Instruments, UK), with a concentration of 0.1 mg/mL. Each value represents the mean + S.D. ($n = 3$).

3.3. Effects of simulated gastric and intestinal fluids on the intracellular uptake of fluorescently labeled silica particles

The effects of dispersion in simulated fluids on the intracellular uptake of silica particles were investigated using Caco-2 cells. In the preliminary experiments, we confirmed that the internalization occur linearly with times around 2 h after the addition of silica particles (Supplementary Fig. 1). Therefore, the intracellular amounts of silica particles were measured after incubation for 2 h with silica particles. Similarly, the silica particle concentrations for incubation were determined based on the linearity between silica particle masses and fluorescent intensities of internalized silica particles (Supplementary Fig. 2). As shown in Fig. 3, the intracellular amounts of SP-50, SP-100, and SP-200 dispersed in fasted-state simulated fluids (FaSSGF and FaSSIF) were almost the same as those in cultured medium (control). However, when SP-50, SP-100, and SP-200 were dispersed in fed-state simulated

Table 3
Stability of fluorescent labeling.

Solution	SP-50	SP-100	SP-200
	Average SD	Average SD	Average SD
MilliQ water	97.8 ± 0.62	99.8 ± 1.40	98.5 ± 4.18
PBS	98.2 ± 1.06	99.3 ± 1.05	98.9 ± 3.55
D-MEM(+)	98.8 ± 0.91	99.5 ± 1.04	98.2 ± 3.34
FaSSIF	99.1 ± 0.53	99.8 ± 1.00	98.4 ± 3.48
FeSSIF	98.4 ± 0.37	99.1 ± 0.68	98.5 ± 2.30
FaSSGF	98.4 ± 0.73	99.0 ± 0.49	98.1 ± 2.56
FeSSGF	97.6 ± 0.61	99.1 ± 0.37	98.5 ± 1.61
Trypsin	98.5 ± 5.90	98.3 ± 7.49	99.9 ± 11.2
Lysis buffer	101.5 ± 5.76	103.8 ± 6.29	99.9 ± 8.63

After incubation of fluorescent labeled silica particles in various solutions, the recovery of fluorescent dye was examined and expressed as percentage of the fluorescent intensity of the resuspended silica particles to that before centrifugation as described in "Materials and methods." Each value represents the mean ± S.D. ($n = 3$).

intestinal fluids (FeSSIF), the measured amounts of intracellular silica particles significantly decreased (Fig. 3). This decrease in the intracellular amounts of silica particles was also observed when the silica particles were serially diluted using FeSSGF and FeSSIF (Fig. 3). We then examined the intracellular uptake of silica particles into Caco-2 cells using confocal microscopy. As shown in Fig. 4 (a), when silica particles were pre-incubated in fasted-state simulated fluids (FaSSIF), the intracellular uptake of silica particles was almost the same as that in PBS. In contrast, when silica particles were pre-incubated in fed-state simulated intestinal fluids (FeSSIF), the intracellular uptake of silica particles significantly decreased (Fig. 4 (a)). This result agreed with the quantitative values obtained using fluorescent spectroscopy described above (Fig. 3). It was also shown that silica particles pre-incubated in PBS and FaSSIF were observed to co-localize with endosomes and lysosomes after incubation for 2 h with Caco-2 cells (Fig. 4 (a)). On the other hand, the internalization of silica particles was not observed when the particles were incubated with Caco-2 cells at 4 °C (Fig. 4 (b)). These indicated that the silica particles were internalized by endocytosis, and that the silica nanoparticles are not simply adhering to the cells.

3.4. Effects of simulated gastric and intestinal fluids on the Caco-2 cell monolayer transport of silica particles

To investigate the effect of various fluids on the transcellular transport of silica particles, SP-50, SP-100, and SP-200 were dispersed in PBS, FaSSIF, and FeSSIF, and silica particle transport studies were performed using Caco-2 cell monolayers (Fig. 5). Fig. 6 shows the time-dependent variations in the TEER and the cumulative amount of transported silica particles dispersed in various types of fluids. The TEER is well known as an indicator of the integrity, or tightness, of junctions (a tight junction is described as the closely associated area between two cells whose membranes have joined together to form a virtually impermeable barrier against various materials) [25]. As shown in Fig. 6, the TEER was hardly affected by the addition of SP-50, SP-100, or SP-200 under these experimental conditions, suggesting that the silica particles used in this study did not significantly change the structure of the tight junctions in the Caco-2 cell monolayers. From the investigation of the cumulative amounts of transported silica particles, it was clear that after 30 min, the transported amounts of SP-50 suspended in PBS and fasted-state fluid were significantly higher than those of SP-50 in fed-state fluid. The transported amounts of SP-50 dispersed in FeSSIF were significantly lower than those of SP-50 dispersed in PBS or fasted-state fluids. In the case of SP-100 and SP-200, the cumulative amount of transported silica particles was negligible until 60 min, even in the PBS and fasted-state fluids (Fig. 6).

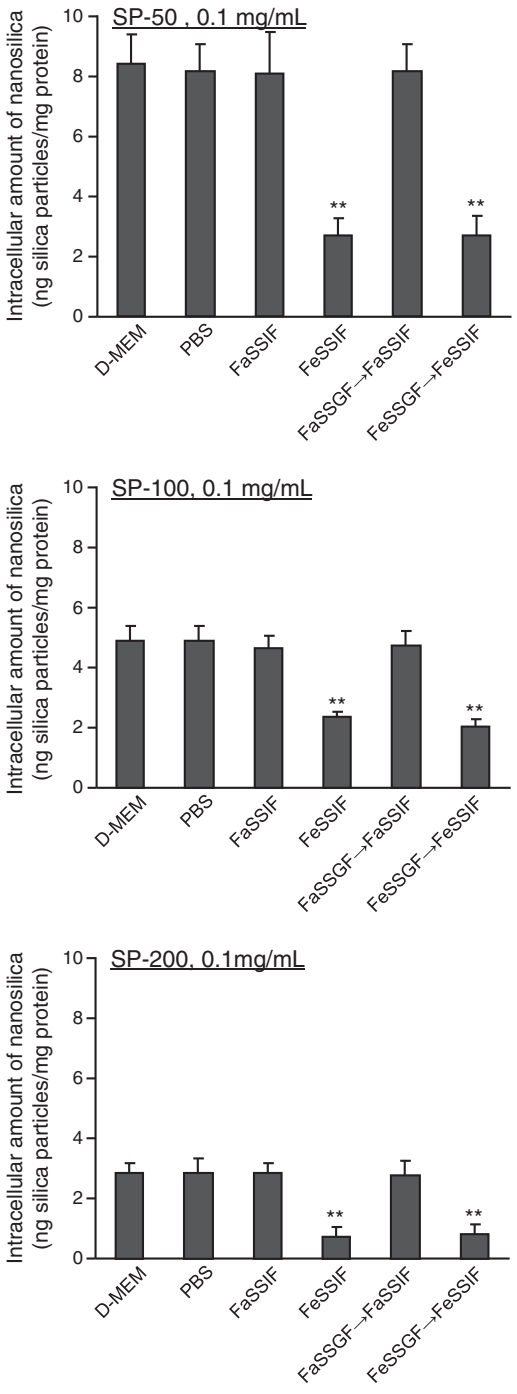

**P<0.01, compared with the corresponding group of D-MEM.

Fig. 3. The intracellular uptake of amorphous silica particles, 2 h after their addition to Caco-2 cells. SP-50, SP-100, and SP-200 were dispersed in various types of fluids and pre-incubated for 1 h. After incubation for 2 h in the silica particle-containing suspension, the cells were then trypsinized, washed, and lysed. The cell suspension was shaken, centrifuged, and the fluorescence intensity of the resulting supernatant was measured as described in Section 2.5. **$P < 0.01$, compared with the corresponding group of D-MEM. Each value represents the mean + S.D. ($n = 6$).

3.5. Effects of simulated gastric and intestinal fluids on the cytotoxicity of silica particles

The effects of various fluids on the cytotoxicity of the silica particles were then evaluated. Silica nanoparticles (final concentration 1.0 mg/mL) were dispersed in various types of fluids and exposed to cells for

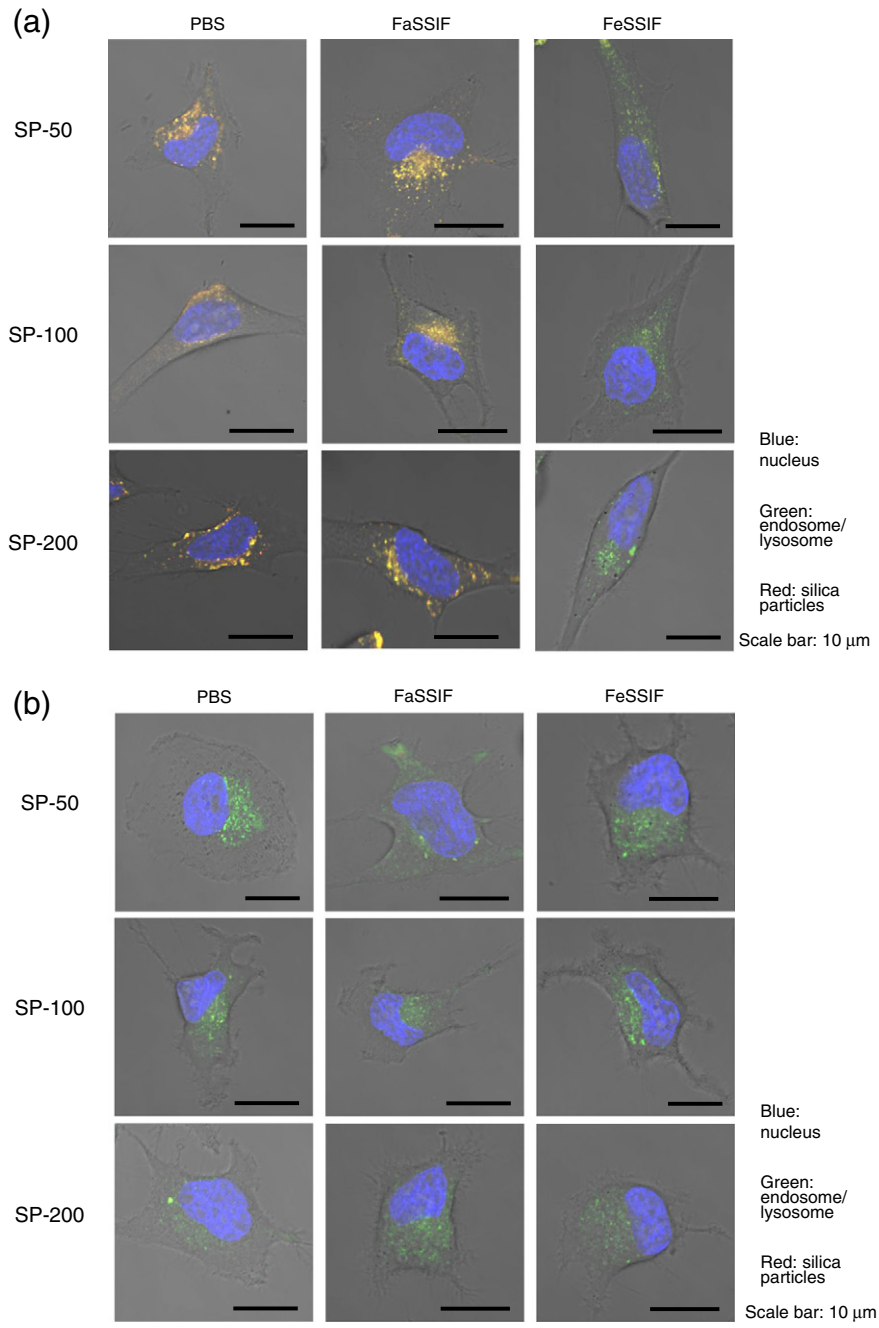

Fig. 4. Confocal images of the intracellular amorphous silica particles, taken 2 h after their addition to Caco-2 cells. The fluorescently labeled silica particles were diluted to a concentration of 0.1 mg/mL in various types of fluids (PBS, FaSSIF, and FeSSIF), and pre-incubated for 1 h to mimic the intestinal conditions. Confocal images of the intracellular amorphous silica particles were taken 2 h after their addition to Caco-2 cells at 37 °C (a) or 4 °C (b). To observe co-localization, endosomes and lysosomes of cells were labeled with AlexaFluor-488-conjugated transferrin and LysoTracker Green DND-26, respectively. The scale bars represent 10 μm.

6 h. Up to this time point, no cytotoxicity was observed in Caco-2 cells exposed to SP-50, SP-100, or SP-200. The cultured media was then replaced with fresh medium without silica particles to eliminate any effect of the fluid itself, and the cells were incubated for another 0, 6, 24, and 48 h (Fig. 7). During this additional incubation with fresh medium, time-dependent toxicity was observed in Caco-2 cells that had been initially exposed to SP-50 dispersed in PBS or fasted-state simulated fluids. By contrast, no cytotoxicity was observed for SP-100 or SP-200 even after 48-h incubation (Fig. 7). We then investigated the concentration dependency of the silica particle toxicity on Caco-2 cells. Silica nanoparticles (final concentration 0.1, 1.0, and 10 mg/mL) were dispersed in various types of fluids and exposed to cells for 6 h. The cultured media was then replaced with fresh medium without silica particles, and the cells were incubated for another 48 h at which time the cytotoxicity of SP-50 was considerable (Fig. 7). As shown in Fig. 8, cytotoxicity was not observed for SP-100 or SP-200 in any of the various types of fluids, even at a concentration of 10 mg/mL. By contrast, when SP-50 was dispersed in PBS or the fasted-state simulated fluids, significant cytotoxicity was detected for all concentrations of the particles, with the cytotoxicity depending on the concentration. However, when SP-50 was dispersed in FeSSIF, cytotoxicity was not observed.

4. Discussion

With the increasing interest in nanotechnology, nanomaterials have been applied in various fields including medicines. Nanoparticles can

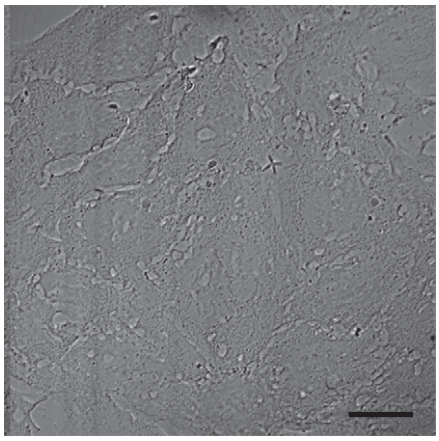

Fig. 5. Phase-contrast image of the Caco-2-cells. The scale bar represents 20 μm.

also be used as excipients of solid oral dosage forms and other products that are absorbed in a body in a variety of ways.

In solid oral dosage form, silicates are commonly used as glidants. Although the primary particle size of the most frequently used colloidal silica (Aerosil 200) is between 7 and 40 nm, these particles group together into so-called aggregates of a few hundred nanometers during the sintering production process [26]. This study therefore investigated the size and in vitro behavior using gastrointestinal models; the Caco-2 cell models and bio-relevant dissolution media simulated conditions in the gastrointestinal system, allowing an evaluation of the intestinal permeability properties and the intestinal cell toxicity associated with oral administration. The critical question regarding the safety of oral dosage forms is whether the material used as an excipient will penetrate the intestinal barrier of the intestinal membrane.

We used fluorescently labeled silica particles to trace the intake and the translocation of the intestinal barrier. The silica particles consisted of amorphous and nonporous silicates, and had a negative charge (Table 1); these characteristics are the same as those of silicates frequently used in solid oral dosage form (approximately −40 mV in

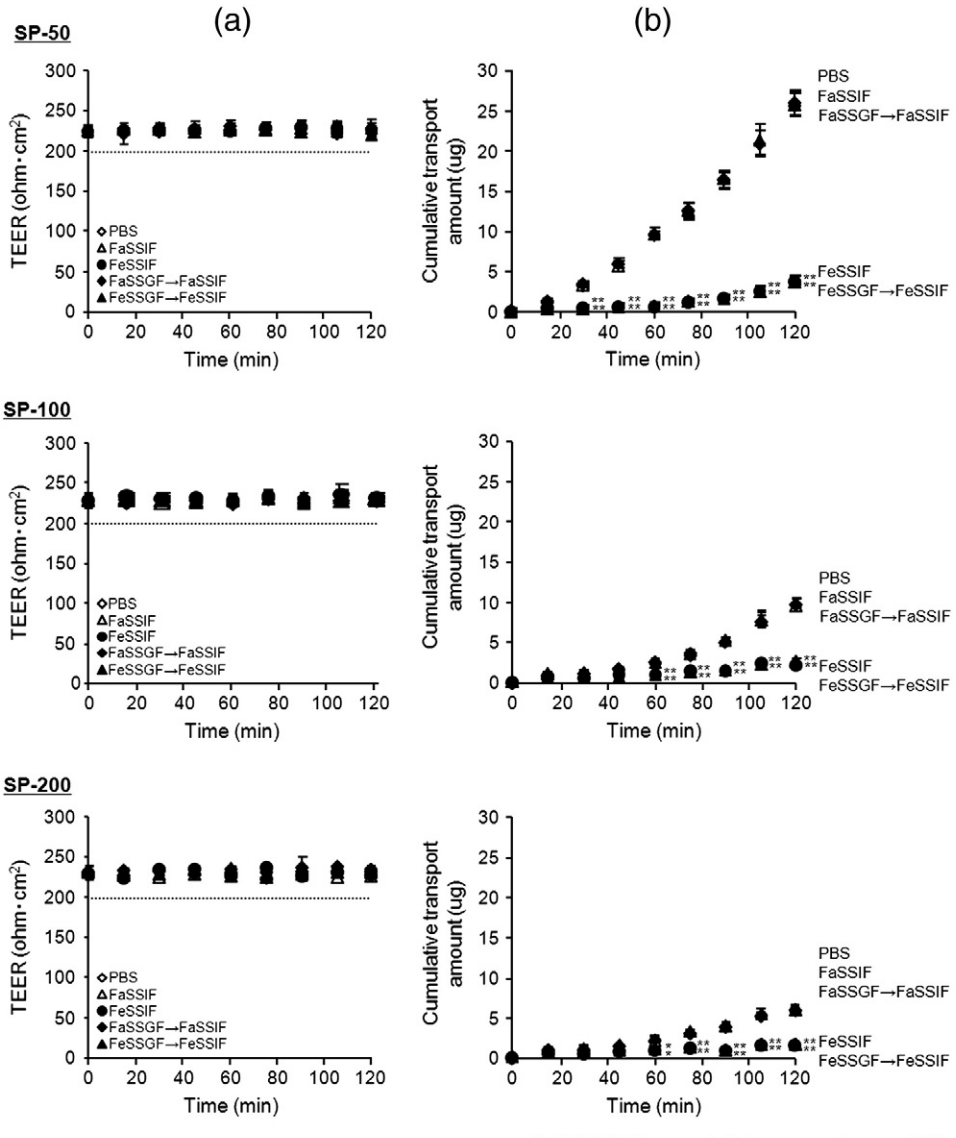

Fig. 6. Trans-epithelial electrical resistance across Caco-2 cell monolayers (a), and cumulative transported amounts of amorphous silica particles (b). SP-50, SP-100, and SP-200 were dispersed in various types of fluids to a final concentration of 1 mg/mL and pre-incubated at 37 °C for 1 h. The incubated fluorescently labeled silica particles were added to the apical side of the Caco-2 cell monolayer. After indicated duration, TEER and the transported amount of nanoparticles were measured as described in "Materials and methods". $^{*}P < 0.05$, $^{**}P < 0.01$, compared with the corresponding group of " PBS". Each value represents the mean ± S.D. ($n = 4$).

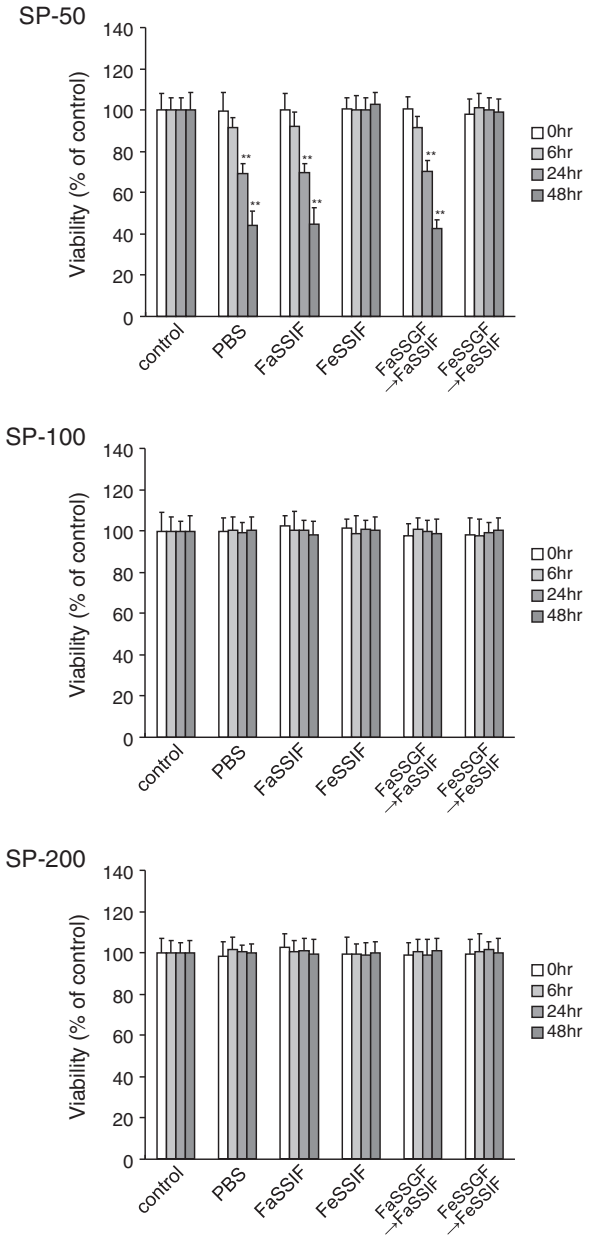

Fig. 7. The cytotoxicity of amorphous silica particles against Caco-2 cells. Silica nanoparticles (final concentration 1.0 mg/mL) were dispersed in various types of fluids and pre-incubated at 37 °C for 1 h. In addition, to mimic the gastric and intestinal conditions (indicated as "FaSSGF → FaSSIF" and "FeSSGF → FeSSIF"), silica particles were diluted to 10 mg/mL in FaSSGF or FeSSGF, incubated at 37 °C for 1 h, and the diluted silica particles were subsequently further diluted to concentrations of 1.0 mg/mL in FaSSIF or FeSSIF, and incubated at 37 °C for an additional 1 h. The pre-incubated particles were added to the cells. After incubation for 6 h, the cultured media was then replaced with fresh medium to eliminate the effect of the fluid itself, and the cells were incubated for another 0, 6, 24, and 48 h. Cell viability was evaluated by using the WST-8 assay at each time point (0, 6, 24, and 48 h). $^{**}P < 0.01$, compared with the corresponding control group. Each value represents the mean ± S.D. ($n = 4$).

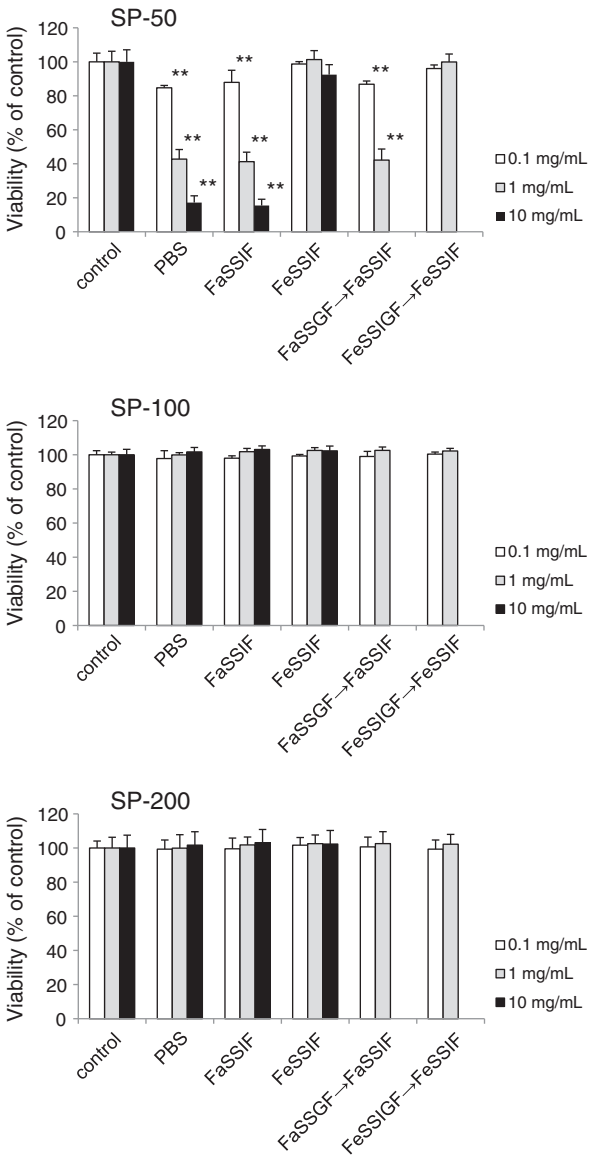

Fig. 8. The concentration dependency of the silica particle toxicity on Caco-2 cells. SP-50, SP-100, and SP-200 (final concentration 0.1, 1.0, and 10 mg/mL) were dispersed in various types of fluids and pre-incubated at 37 °C for 1 h. In addition, to mimic the gastric and intestinal conditions (indicated as "FaSSGF → FaSSIF" and "FeSSGF → FeSSIF"), silica particles were diluted to 10 mg/mL in FaSSGF or FeSSGF, incubated at 37 °C for 1 h, and the diluted silica particles were subsequently further diluted to concentrations of 0.1 or 1.0 mg/mL in FaSSIF or FeSSIF, and incubated at 37 °C for an additional 1 h. The pre-incubated particles were added to the cells. After incubation for 6 h, the cultured media was then replaced with fresh medium to eliminate the effect of the fluid itself, and an additional 48 h of incubation was applied, followed by measurement of cytotoxicity. $^{**}P < 0.01$, compared with the corresponding control group. Each value represents the mean ± S.D. ($n = 4$).

water at pH 7 [27]). We also investigated the size dependence of the absorption and the in vitro toxicity, using silica particles with diameters of 50, 100, and 200 nm.

First, we investigated whether the silica particles would agglomerate after oral administration. Simulation of gastrointestinal conditions is essential to adequately predict the in vivo behavior of drug formulations. We used biorelevant dissolution media that can be used for the in vitro simulation of different dosing conditions (fasted and fed states) [28]. Regardless of the primary particle size, the observed tendency was the same. In all cases, the particles formed agglomerates in the medium representing the fed-state intestinal fluid. It is known that acidic conditions promote agglomeration, due to a decrease in the electrostatic repulsion between negatively charged silica particles; the formation of agglomerates can therefore occur after passage through the stomach, which has lower-pH conditions. However, in this case, lower-pH conditions did not cause agglomeration, under fed or fasted conditions. Furthermore, the viscosity of the FaSSGF = 0.688 mPa s and FeSSGF = 0.704 mPa s were almost the same, which suggested that the viscosity did not affect the agglomeration of the silica particles. Judging from the composition of the bio-relevant dissolution media, and the above results, we concluded that the high salt concentration was a major factor causing the agglomeration. In fact, we reported previously

that silica particles easily agglomerated with high sodium ion concentrations in solution eluents [29], and the same phenomenon was also reported by other researchers [30]. The Derjaguin Landau_Verwey_Overbeek (DLVO) theory is often used to explain the aggregation/agglomeration behavior of silica suspensions [31,32]. Briefly, the DLVO theory combines the effects of the attractive van der Waals forces and the electrostatic repulsion between charged surfaces. As discussed earlier, the presence of silanol groups (Si–O–H) on amorphous silica surfaces and the charge of silanol groups determine the extent of the repulsive energy needed to keep the silica nanoparticles dispersed. The surface charge of silica nanoparticles differs as the pH changes due to protonation and deprotonation of the silanol groups. At pH 2–3, silica nanoparticles reach the isoelectric point (IEP) where the particles carry no net charge, causing the nanoparticles to agglomerate. In the case of biological conditions with high (0.1–0.3 M) salt concentrations, ion-specific effects also play a prominent role [33]. Amiri et al. pointed out that in aqueous media, because pure particles are electrostatically stabilized, interparticle interactions at a given concentrations can be changed by varying the ionic strength, particle size, and pH of the suspension; they demonstrated that high salt concentration causes agglomeration of silica particles [27].

Next, we studied the cellular uptake of silica particles, using Caco-2 cells as an in vitro model to assess the barrier integrity/permeability effects of the silica particles. The TEER, which is well known as an indicator of the integrity of junctions, was not affected by the addition of SP-50, SP-100, or SP-200 under these experimental conditions, suggesting that the silica particles used in this study did not significantly change the structure of the tight junctions between the cells in the Caco-2 cell monolayer, regardless of the particle size, at least for 2 h of exposure to the particles. Because the length of the tight junction between the cells is approximately 10–20 nm [25], the silica particles used in this study did not penetrate the junction. Therefore, the increase in the amount of particles showed that translocation through the Caco-2 cells occurred. The transport experiments showed that the cumulative number of transported silica particles increased with exposure time, and it is notable that translocation occurred under conditions that did not cause agglomeration. In the investigation of the cumulative amount of transported silica particles, Fig. 6 showed that the transported amounts of SP-50 were much higher than those of SP-100 and 200 when these silica particles were dispersed in PBS and FaSSIF. Moreover, the transported amounts of all of the silica particles were significantly lower when they were dispersed in FeSSIF than when they were dispersed in PBS or FaSSIF. However, in the case of SP-100 and SP-200, the amounts of silica particles transported were negligible for times shorter than 1 h, regardless of which fluid was used. Because the transit time in the gut is approximately 1 h per 1 m of gut length [34], these results suggest that the intestinal absorption of silica particles or aggregates/agglomerates larger than 100 nm would be negligible. Further in vivo testing would be necessary to confirm the possibility of silica particle absorption into the systemic circulation.

We then investigated the cytotoxicity of the silica particles towards Caco-2 cells. We confirmed that the exposure for 6 h to the silica particles (SP-50,100, and 200) did not induce cytotoxicity in any of the various types of fluids, and this coincides with our results that the structure of the tight junctions of Caco-2 monolayer was not changed at least for 2 h of exposure to the silica particles (Fig. 6). However, after another incubation with fresh medium, SP-50 showed time-dependent toxicity for up to 48 h when SP-50 was dispersed in PBS or fasted-state simulated fluids. On the other hand, SP-100 and SP-200 did not show any cytotoxicity, at least for 48 h (Fig. 7). The time lapse of toxicity observed in SP-50 in this study indicates that the smaller size of silica particles inhibited cellular proliferation, which has also been reported by Nabeshi et al. [35]. They showed the size-dependent cytotoxic effects of amorphous silica particles (70, 300, and 1000 nm) on mouse epidermal Langerhans cells. The smallest particles induced greater cytotoxicity and inhibited cellular proliferation [35]. We investigated the concentration dependency of silica particles on Caco-2 cells and found that SP-50 was cytotoxic. No cytotoxicity was observed, however, for SP-100 or SP-200, in any of the various types of fluids, even at a concentration of 10 mg/mL (Fig. 8). By contrast, when SP-50 was dispersed in PBS or fasted-state simulated fluids, significant cytotoxicity was detected for all concentrations of the particles, with increasing cytotoxicity as the silica concentration increased. Although SP-100 and 200 were also internalized in the Caco-2 cells in the fasted state, cytotoxicity was not observed.

The size-dependent toxicity of amorphous nanosilica has been also reported by other researchers [16]. The relationship between cytotoxicity and particle sizes observed in our study has been discussed previously by others. Yu et al. examined the cytotoxic activity of well-dispersed amorphous silica particles (30–535 nm) in mouse keratinocytes [36]. All sizes of particles were taken up into the cell cytoplasm. The toxicity was dose- and size-dependent, with 30- and 48-nm particles being more cytotoxic than 118- and 535-nm particles. Nabeshi et al. showed the size-dependent cytotoxic effects of amorphous silica particles (70, 300, and 1000 nm) on mouse epidermal Langerhans cells [35]. They found that the smallest particles induced the greatest cytotoxicity and inhibited cellular proliferation. These observed effects were associated with the quantity of particle uptake into the cells. This association was also present in our study, where the cytotoxicity of SP-50 correlated with the concentration (Fig. 8). Yang et al. evaluated the effects of amorphous silica particles (15 and 30 nm) on cellular viability, the cell cycle, and apoptosis in the human epidermal keratinocyte cell line HaCaT [37]. Their microscopic examination revealed morphological changes after 24-h exposures. Cell growth also appeared to be significant inhibited, and the smaller silica particles were more cytotoxic and induced a higher rate of apoptosis. Oberdörster et al. argued that since smaller particles have a bigger surface area per unit of mass, the surface area is a pivotal factor for the displayed biological activity [38]. The mechanisms by which silica particles exert their cytotoxic effects are still largely unknown, and recent research illustrates the complexity in identifying the hazards of nanoparticles for human health [39]. However, there are many possibilities, including damage to the plasma membrane before particles penetrate the cells, intracellular interference after uptake in late or lysosomal structures, and lysosomal escape [16]. Another research indicated that the effect of silica nanoparticles on HT-29 cells is mediated by the interference with the signaling pathway such as MAPK/ERK1/2 [40].

Our study showed that when SP-50 was dispersed in FeSSIF, large agglomerates were formed, and cytotoxicity was not observed. This indicated that even if the primary particle size was less than 100 nm, the cytotoxicity was largely affected by the agglomerate formation.

Guidance for the assessment of risks associated with the application of nanoscience and nanotechnologies in the food and feed chain [41] recommends in vitro tests, including assessments of the effect of particles on the integrity of the gastrointestinal barriers. Our studies proposed one model to assess the integrity/permeability of the gastrointestinal barrier, and the cytotoxicity based on differentiated Caco-2 cells. Parameters such as the cell viability and the TEER can be also considered to be recommended in the guidance.

5. Conclusions

In the present study, we developed the in vitro assay systems including cellular uptake, transport study, and cytotoxicity study models using Caco-2 cells and simulated gastrointestinal fluids to help the evaluation of the intestinal permeability properties and intestinal cell toxicity of silica particles after they were administered orally. Our study showed that the agglomeration of silica particles was affected by the diet and gastrointestinal fluids. Our study also indicated that there was no significant penetration of silica particles through in vitro models (Caco-2 cells), and the cytotoxicity was not observed if the mean size was larger than 100 nm. This study further showed that the secondary size, including

the factor of agglomeration, is important to assess the potential harmful effects of silica particles on Caco-2 cells. Even when the primary particle size was less than 100 nm, the cytotoxicity was affected by agglomerate formation. The findings obtained from our study may offer valuable information to evaluate the behavior in the gastrointestinal tracts or safety of medicines or foods containing silica particles as additives.

Supplementary data to this article can be found online at http://dx.doi.org/10.1016/j.bbagen.2013.12.014.

Acknowledgement

This work was supported in part by the Health and Labour Sciences Research Grants from the Ministry of Health, Labour and Welfare of Japan.

References

[1] A.B. Lansdown, A. Taylor, Zinc and titanium oxides: promising UV-absorbers but what influence do they have on the intact skin? Int. J. Cosmet. Sci. 19 (1997) 167–172.
[2] H. Nabeshi, T. Yoshikawa, K. Matsuyama, Y. Nakazato, K. Matsuo, A. Arimori, M. Isobe, S. Tochigi, S. Kondoh, T. Hirai, T. Akase, T. Yamashita, K. Yamashita, T. Yoshida, K. Nagano, Y. Abe, Y. Yoshioka, H. Kamada, T. Imazawa, N. Itoh, S. Nakagawa, T. Mayumi, S. Tsunoda, Y. Tsutsumi, Systemic distribution, nuclear entry, and cytotoxicity of amorphous nanosilica following topical application, Biomaterials 32 (2011) 2713–2724.
[3] A. Kunzmann, B. Andersson, T. Thurnherr, H. Krug, A. Scheynius, B. Fadeel, Toxicology of engineered nanomaterials: focus on biocompatibility, biodistribution, and biodegradation, Biochim. Biophys. Acta 1810 (2011) 361–373.
[4] A.M. Nyström, B. Fadeel, Safety assessment of nanomaterials: implications for nanomedicine, J. Control. Release 161 (2012) 403–408.
[5] M. Ferrari, Cancer nanotechnology: opportunities and challenges, Nat. Rev. Cancer 5 (2005) 161–171.
[6] Y. Malam, M. Loizidou, A.M. Seifalian, Liposomes and nanoparticles: nanosized vehicles for drug delivery in cancer, Trends Pharmacol. Sci. 30 (2009) 592–599.
[7] N. Nishiyama, K. Kataoka, Current state, achievements, and future prospects of polymeric micelles as nanocarriers for drug and gene delivery, Pharmacol. Ther. 112 (2006) 630–648.
[8] R.A. Petros, J.M. DeSimone, Strategies in the design of nanoparticles for therapeutic applications, Nat. Rev. Drug Discov. 9 (2010) 615–627.
[9] C.M. Hentzschel, M. Alnaief, I. Smirnova, A. Sakmann, C.S. Leopold, Tableting properties of silica aerogel and other silicates, Drug Dev. Ind. Pharm. 38 (2012) 462–467.
[10] L. Jia, J. Shen, Z. Li, D. Zhang, Q. Zhang, G. Liu, D. Zheng, X. Tian, In vitro and in vivo evaluation of paclitaxel-loaded mesoporous silica nanoparticles with three pore sizes, Int. J. Pharm. 445 (2013) 12–19.
[11] H. Miura, M. Kanebako, H. Shirai, H. Nakao, T. Inagi, K. Terada, Influence of particle design on oral absorption of poorly water-soluble drug in a silica particle–supercritical fluid system, Chem. Pharm. Bull. 59 (2011) 686–691.
[12] M.D. Popova, A. Szegedi, I.N. Kolev, J. Mihaly, B.S. Tzankov, G.T. Momekov, N.G. Lambov, K.P. Yoncheva, Carboxylic modified spherical mesoporous silicas as drug delivery carriers, Int. J. Pharm. 436 (2012) 778–785.
[13] P.J. Borm, D. Robbins, S. Haubold, T. Kuhlbusch, H. Fissan, K. Donaldson, R. Schins, V. Stone, W. Kreyling, J. Lademann, J. Krutmann, D. Warheit, E. Oberdorster, The potential risks of nanomaterials: a review carried out for ECETOC, Part. Fibre Toxicol. 3 (2006) 11.
[14] K.M. Waters, L.M. Masiello, R.C. Zangar, B.J. Tarasevich, N.J. Karin, R.D. Quesenberry, S. Bandyopadhyay, J.G. Teeguarden, J.G. Pounds, B.D. Thrall, Macrophage responses to silica nanoparticles are highly conserved across particle sizes, Toxicol. Sci. 107 (2009) 553–569.
[15] T. Hirai, T. Yoshikawa, H. Nabeshi, T. Yoshida, S. Tochigi, K. Ichihashi, M. Uji, T. Akase, K. Nagano, Y. Abe, H.K. amada, N. Itoh, S. Tsunoda, Y. Yoshioka, Y. Tsutsumi, Amorphous silica nanoparticles size-dependently aggravate atopic dermatitis-like skin lesions following an intradermal injection, Part. Fibre Toxicol. 9 (2012) 3.
[16] J. Kasper, M.I. Hermanns, C. Bantz, O. Koshkina, T. Lang, M. Maskos, C. Pohl, R.E. Unger, C.J. Kirkpatrick, Interactions of silica nanoparticles with lung epithelial cells and the association to flotillins, Arch. Toxicol. 87 (2012) 1053–1065.
[17] M. Pinto, S. Robine-Leon, M.D. Appay, M. Kedinger, N. Triadou, I. Dussaulx, B. Lacroix, P. Simon-Assmann, K. Haffen, J. Fogh, A. Zweibaum, Enterocyte-like differentiation and polarization of the human colon carcinoma cell line Caco-2 in culture, Biol. Cell 47 (1983) 323–330.
[18] I.J. Hidalgo, T.J. Raub, R.T. Borchardt, Characterization of the human colon carcinoma cell line (Caco-2) as a model system for intestinal epithelial permeability, Gastroenterology 96 (1989) 736–749.
[19] P. Artursson, J. Karlsson, Correlation between oral drug absorption in humans and apparent drug permeability coefficients in human intestinal epithelial (Caco-2) cells, Biochem. Biophys. Res. Commun. 175 (1991) 880–885.
[20] K. Gerloff, C. Albrecht, A.W. Boots, I. Forster, R.P.F. Schins, Cytotoxicity and oxidative DNA damage by nanoparticles in human intestinal Caco-2 cells, Nanotoxicology 3 (2009) 355–364.
[21] N. Reix, A. Parat, E. Seyfritz, R. Van der Werf, V. Epure, N. Ebel, L. Danicher, E. Marchioni, N. Jeandidier, M. Pinget, Y. Frere, S. Sigrist, In vitro uptake evaluation in Caco-2 cells and in vivo results in diabetic rats of insulin-loaded PLGA nanoparticles, Int. J. Pharm. 437 (2012) 213–220.
[22] V. Uskoković, K. Lee, P.P. Lee, K.E. Fischer, T.A. Desai, Shape effect in the design of nanowire-coated microparticles as transepithelial drug delivery devices, ACS Nano 6 (2012) 7832–7841.
[23] E. Jantratid, N. Janssen, C. Reppas, J.B. Dressman, Dissolution media simulating conditions in the proximal human gastrointestinal tract: an update, Pharm. Res. 25 (2008) 1663–1676.
[24] V.G. DeMarco, N. Li, J. Thomas, C.M. West, J. Neu, Glutamine and barrier function in cultured Caco-2 epithelial cell monolayers, J. Nutr. 133 (2003) 2176–2179.
[25] J.M. Anderson, Molecular structure of tight junctions and their role in epithelial transport, News Physiol. Sci. 16 (2001) 126–130.
[26] Evonik Industries: Technical Information No. 1271.
[27] A. Amiri, G. Oye, J. Sjoblom, Influence of pH, high salinity, and particle concentration on stability and rheological properties of aqueous suspensions of fumed silica, Colloids Surf. A Physicochem. Eng. Asp. 349 (2009) 43–54.
[28] S. Klein, The use of biorelevant dissolution media to forecast the in vivo performance of a drug, AAPS J. 12 (2010) 397–406.
[29] K. Sakai-Kato, S. Ota, T. Takeuchi, T. Kawanishi, Size separation of colloidally dispersed nanoparticles using a monolithic capillary column, J. Chromatogr. A 1218 (2011) 5520–5526.
[30] J. Depasse, A. Watillon, The stability of amorphous colloidal silica, J. Colloid Interface Sci. 33 (1970) 430–438.
[31] E.J.W. Verwey, J.T.G. Overbeek, Theory of the Stability of Lyophobic Colloids, Elsevier, Amsterdam, 1948.
[32] B. Derjaguin, L. Landau, Theory of the stability of strongly charged lyophobic sols and of the adhesion of strongly charged particles in solution of electrolytes, Acta Phys.-Chim. 14 (1941) 633–662(URSS).
[33] R. Peters, E. Kramer, A.G. Oomen, Z.E. Rivera, G. Oegema, P.C. Tromp, R. Fokkink, A. Rietveld, H.J. Marvin, S. Weigel, A.A. Peijnenburg, H. Bouwmeester, Presence of nano-sized silica during in vitro digestion of foods containing silica as a food additive, ACS Nano 6 (2012) 2441–2451.
[34] N. Parrott, V. Lukacova, G. Fraczkiewicz, M.B. Bolger, Predicting pharmacokinetics of drugs using physiologically based modeling-application to food effects, AAPS J. 11 (2009) 45–53.
[35] H. Nabeshi, T. Yoshikawa, K. Matsuyama, Y. Nakazato, A. Arimori, M. Isobe, S. Tochigi, S. Kondoh, T. Hirai, T. Akase, T. Yamashita, K. Yamashita, T. Yoshida, K. Nagano, Y. Abe, Y. Yoshioka, H. Kamada, T. Imazawa, N. Itoh, S. Tsunoda, Y. Tsutsumi, Size-dependent cytotoxic effects of amorphous silica nanoparticles on Langerhans cells, Pharmazie 65 (2010) 199–201.
[36] K.O. Yu, C.M. Grabinski, A.M. Schrand, R.C. Murdock, W. Wang, B. Gu, J.J. Schlager, S.M. Hussain, Toxicity of amorphous silica nanoparticles in mouse keratinocytes, J. Nanopart. Res. 11 (2009) 15–24.
[37] X. Yang, J. Liu, H. He, L. Zhou, C. Gong, X. Wang, L. Yang, J. Yuan, H. Huang, L. He, B. Zhang, Z. Zhuang, SiO2 nanoparticles induce cytotoxicity and protein expression alteration in HaCaT cells, Part. Fibre Toxicol. 7 (2010) 1–12.
[38] G. Oberdörster, E. Oberdörster, J. Oberdörster, Nanotoxicology: an emerging discipline evolving from studies of ultrafine particles, Environ. Health Perspect. 113 (2005) 823–839.
[39] J.A. Sergent, V. Paget, S. Chevillard, Toxicity and genotoxicity of nano-SiO2 on human epithelial intestinal HT-29 cell line, Ann. Occup. Hyg. 56 (2012) 622–630.
[40] H. Gehrke, A. Frühmesser, J. Pelka, M. Esselen, L.L. Hecht, H. Blank, H.P. Schuchmann, D. Gerthsen, C. Marquardt, S. Diabaté, C. Weiss, D. Marko, In vitro toxicity of amorphous silica nanoparticles in human colon carcinoma cells, Nanotoxicology 7 (2013) 274–293.
[41] EFSA Scientific Committee, Scientific opinion: guidance on the risk assessment of the application of nanoscience and nanotechnologies in the food and feed chain, EFSA J. 9 (2011) 2140.